



## Structural, Optical, and Humidity Sensing Performance of Pb-Doped ZnO Nanostructure Prepared by Sol-Gel Immersion Method

A.S. Ismail<sup>1</sup>, M.H. Mamat<sup>1,2</sup>, M.M. Yusoff<sup>1</sup>, M.F. Malek<sup>1,2</sup>, A.S. Zoolfakar<sup>1</sup>, R. Mohamed<sup>1</sup>, N.D. Md. Sin<sup>1</sup>, W.R.W. Ahmad<sup>1</sup>, A.B. Suriani<sup>3</sup>, M.K. Ahmad<sup>4</sup>, I.B. Shameem Banu<sup>5</sup>, and M. Rusop<sup>1,2</sup>

<sup>1</sup>NANO-ElecTronic Centre (NET), Faculty of Electrical Engineering, Universiti Teknologi MARA (UiTM), 40450, Shah Alam, Selangor, Malaysia, [mhmamat@salam.uitm.edu.my](mailto:mhmamat@salam.uitm.edu.my),

<sup>2</sup>NANO-SciTech Centre, Institute of Science, Universiti Teknologi MARA, 40450, Shah Alam, Selangor, Malaysia

<sup>3</sup>Faculty of Science and Mathematics, Universiti Pendidikan Sultan Idris, Tanjung Malim, Perak 35900, Malaysia.

<sup>4</sup>Microelectronic and Nanotechnology – Shamsuddin Research Centre (MiNT-SRC), Faculty of Electrical and Electronic Engineering, Universiti Tun Hussein Onn Malaysia (UTHM), 86400 Batu Pahat, Johor, Malaysia

<sup>5</sup>Department of Physics, B.S. Abdur Rahman Crescent Institute of Science & Technology, Vandalur, Chennai 600 048, India. [mhmamat@salam.uitm.edu.my](mailto:mhmamat@salam.uitm.edu.my)

### ABSTRACT

Lead (Pb)-doped zinc oxide (ZnO) nanostructured film was prepared using sol-gel immersion method. The surface morphology of the ZnO films displayed a significant change in structure after doped with Pb. The diameter of the nanostructures was increased from 50 nm to 80 nm after doped. Besides, the crystallinity of the film was improved after doped with Pb, as well as the crystallite size of the Pb-doped ZnO film. The Pb-doped ZnO film showed excellent transmittance properties with average transmittance of 83%. Pb-doped sample displayed better absorbance than that of undoped ZnO at UV region and also have high optical band gap energy of 3.27 eV. In addition, Pb-doped ZnO film exhibited a stable response to humidity change with a sensitivity of 1.21.

**Key words :** ZnO nanostructure, Pb-doped, immersion, humidity sensor.

### 1. INTRODUCTION

Nowadays, zinc oxide (ZnO) has been widely studied for various kinds of applications due to its characteristics such as non-toxic, wide band gap of 3.37 eV and exciton binding energy of 60 meV [1, 2]. Fabrication of ZnO in nanostructure scale is considerably importance due to high surface-to-volume ratio, small size, and better device performance [3, 4]. ZnO nanostructures can be synthesized through many kinds of preparation methods such as immersion, chemical vapor deposition, electron beam evaporation, and electrochemical-deposition methods [5-7]. Between the processes, immersion is one of the most commonly used. The preparation of ZnO nanorod arrays through a simple sol-gel method such as immersion usually produce device with high resistivity [8]. The adjustment on

conductivity of the ZnO nanorods is crucial to improve their capability as a device for example through doping process with different kind of metal such as aluminium (Al), ferum (Fe), magnesium (Mg), and tin (Sn) [9, 10]. In this research, effect of lead (Pb) doping on the structural and optical properties of ZnO is discussed, together with their performance in humidity sensing. Although, ZnO nanorod properties were widely discussed in the literatures, effects of Pb doping into ZnO were rarely discussed in details especially for humidity sensing performance. Therefore, it is worth to investigate this topic to understand Pb-doped ZnO behaviour in term of their structural, optical, and humidity sensing performance.

### 2. EXPERIMENTAL PROCEDURES

The development of the ZnO nanostructures film was built up by means of the sol-gel submersion technique onto Al-doped ZnO covered glass substrate. The detail arrangement has been accounted for somewhere else [11]. The ZnO seed layer arrangement was readied utilizing zinc acetic acid derivation dry out, aluminum nitrate and monoethanolamine. The readied arrangement was saved onto a glass substrate utilizing a turn covering strategy. The answer for developing nanostructured ZnO was readied utilizing zinc nitrate hexahydrate as a forerunner, hexamethylenetetramine as the stabilizer, aluminum nitrate nonahydrate as the dopant, and deionized (DI) water as the dissolvable.

The solution was sonicated using ultrasonic water bath and then stirrer for 3 hours. Then the sample was immersed in water bath tank for 1 hour to grow the Pb-doped ZnO nanostructures. After deposition, the film was dried and annealed at 500 °C. Gold (Au) was coated on the film as metal contact. The synthesis of Pb-doped ZnO nanostructures is illustrated in Fig. 1. Field-emission scanning electron microscopy (FESEM, JEOL JSM-7600F), X-ray diffraction (XRD; PANalytical X'Pert PRO), and energy-dispersive

X-ray spectroscopy (EDS, Oxford Instruments Inca X-Act) were used to analysed the structural properties and elemental analysis of the films. UV-Vis-NIR spectrophotometer (Cary 5000) were used to observe the transmittance and absorbance of the films. Humidity sensor measurement system (Keithley 2400) were used to study the humidity sensing performance of the films.

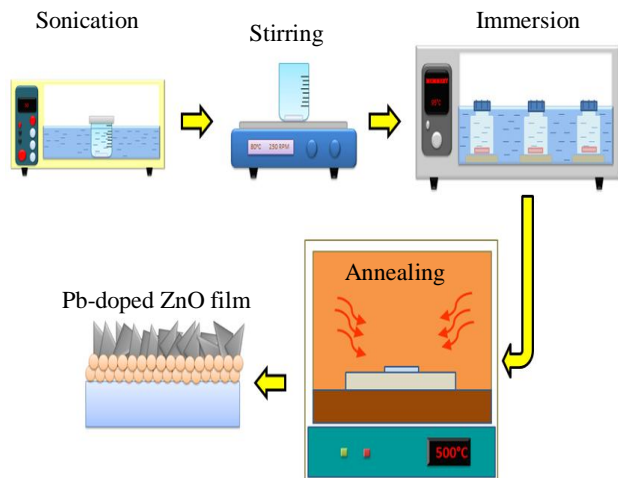
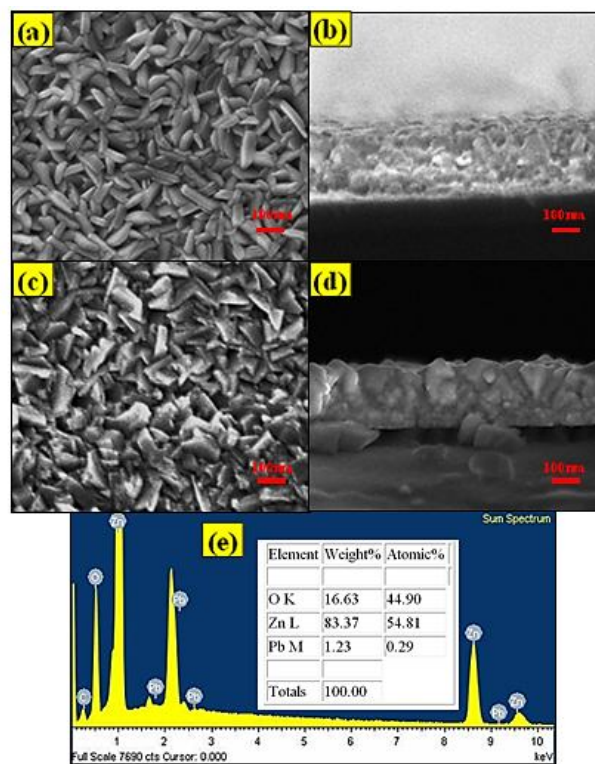


**Figure 1:** Preparation of Pb-doped nanostructures

### 3. EXPERIMENTAL RESULT

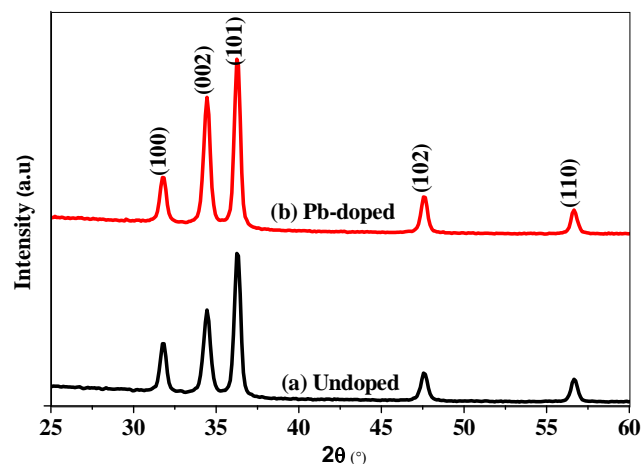
#### 3.1. Structural Properties

Fig. 2 shows the surface and cross-sectional images of undoped and Pb-doped ZnO nanorod arrays. Undoped ZnO sample exhibits rice-like structure with average diameter about 50 nm and thickness about 200 nm, whereas Pb-doped ZnO sample exhibits triangle-shape nanostructures with average diameters about 80 nm and thickness about 200 nm. Both films are highly dense and has low pore channel in between the nanostructures. In addition, the increment of diameter after Pb doping may due to substitution of larger ionic radius of  $Pb^{2+}$  (1.19 Å) replacing the  $Zn^{2+}$  (0.74 Å) sites [12, 13]. The elemental analysis in Fig. 2(e) confirms the availability of Pb atoms in the ZnO structure. According to the elemental analysis, the percentages of zinc (Zn), oxygen (O), and Pb are 54.81%, 44.90%, and 0.29%, respectively.



**Figure 2:** (a) Surface and (b) cross-sectional images of undoped ZnO. (c) Surface and (d) cross-sectional images of Pb-doped ZnO. (e) Elemental analysis of Pb-doped ZnO

The structural properties of the films were further analyzed using XRD measurement as shown in Fig. 3. The XRD pattern showed that the films consist of ZnO hexagonal wurtzite structure with polycrystalline structure. The XRD peaks of both samples are correspond to (100), (002), (101), (102), and (110) of ZnO plane orientations with (101) plane displayed the highest intensity. No additional PbO peak can be observed which indicates that the film is purely ZnO. Besides, we observed an enhancement of peak intensity especially for (002) plane which indicates that doping with Pb manage to improve the crystallinity of the ZnO film.



**Figure 3:** XRD pattern of (a) undoped and (b) Pb-doped ZnO

The average crystallite sizes were acquired from the given equation [14]:

$$D = \frac{0.94\lambda}{\beta \cos\theta} \tag{1}$$

Here,  $D$  is the crystallite size,  $\lambda$  is the X-rays wavelength used,  $\beta$  is the line broadening at Full Width at Half Maximum intensity (FWHM), and  $\theta$  is the Bragg diffraction angle. The values of  $\beta$  and  $\theta$  for undoped ZnO are recorded to be  $0.4804^\circ$  and  $17.22^\circ$ , respectively, meanwhile for Pb-doped ZnO are  $0.4480^\circ$  and  $17.22^\circ$ , respectively. From the calculation, the average crystallite size of undoped and Pb-doped ZnO is estimated to be 18.1 and 19.4 nm, respectively. The increment of crystallite size may be provided by the substitution of larger ionic radius of  $Pb^{2+}$  into ZnO structure [12]. This finding is in agreement with the observation of FESEM images. On the basis of previous study, doping with Pb causes an increment of nanostructure sizes, leading to a film with lower stress [14]. As a result, the crystallinity of the film is improved.

### 3.2. Optical Properties

The optical properties of the films are shown in Fig. 4. Both samples exhibit good transmittance properties (Fig. 4(a)) in the visible region with average transmittance around 83%. No significant changes to the transmittance properties after doped with Pb. Meanwhile, the absorbance of Pb-doped sample is slightly higher than that of undoped ZnO at UV region (Fig. 4(b)). This increment of absorbance may be due to increment of optical scattering effect in the film provided by the enlargement of nanostructure size.

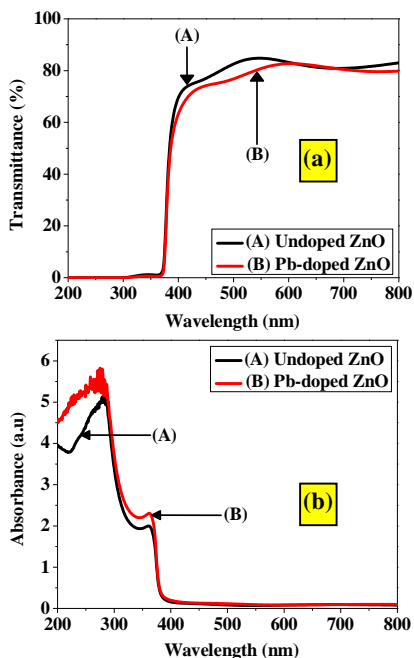


**Figure 4:** (a) Transmittance and (b) absorbance properties of undoped ZnO and Pb-doped ZnO

The optical band energy of the films was estimated using the following equation [15]-[16]:

$$ahv = B(hv - E_g)^{\frac{1}{2}} \tag{2}$$

where  $\alpha$ ,  $h\nu$ ,  $E_g$ , and  $B$  are the absorption coefficient, photon energy, optical band gap energy, and energy-independent constant, respectively. The Tauc's plot is shown in Fig. 5. The estimated energy gap of the films is approximately 3.27 eV, which is close to the band gap energy of intrinsic ZnO (3.37 eV). No changes to the energy gap can be observed after doping with Pb. This may due to the similar thickness of both films and also no increment to the carrier concentration which leads to band gap shifting, in accordance to Burstein–Moss effect [8].

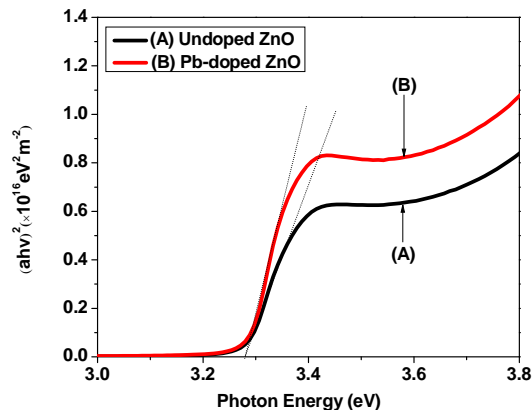


**Figure 5:** Tauc's plot for optical band gap energy estimations

### 3.3. Humidity Sensor Performance

The humidity sensor performance of undoped and Pb-doped ZnO-based humidity sensors can be observed in Fig. 6. The undoped ZnO-based humidity sensor displayed a gradual increase in current signal with slow response from 40% to 90% RH. However, Pb-doped ZnO-based humidity sensor produced high current signal change at low humidity level and then increased slowly when humidity level almost reaching 90% RH. The sensitivities of the undoped- and Pb-doped ZnO-based humidity sensors are estimated using the following equation [17]:

$$S = \frac{R_a}{R_{rh}} \tag{3}$$

Here,  $S$  is the sensitivity,  $R_a$  and  $R_{rh}$  are the resistance at 40% and 90% RH, respectively. From the response curve, the sensitivities of undoped and Pb-doped ZnO-based humidity sensors are estimated to be 1.18 and 1.21, respectively. Other than sensitivity, it is observed that the response curve of Pb-doped sample possessed a smoother and stable current signal than that of undoped sample. The slight increment of sensitivity and stable adsorption/desorption processes may be due to better electron transport properties across the film of Pb-doped ZnO film which possesses larger crystallite size. These results suggested that the performance and certain properties of ZnO nanostructures can be improved by doping with Pb.

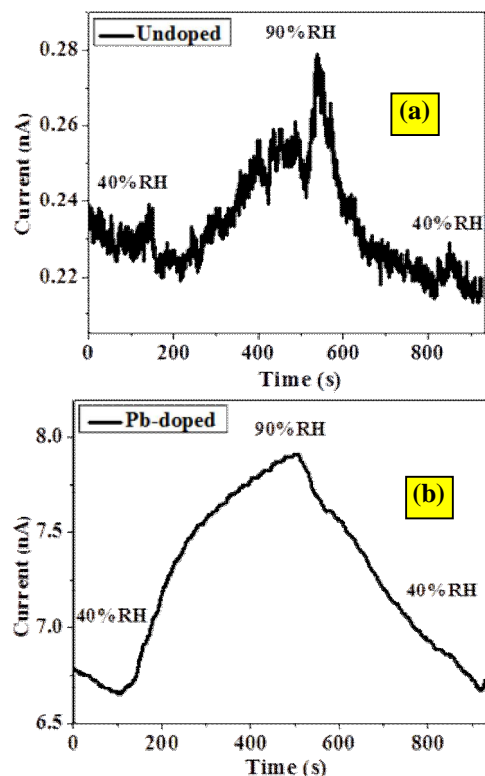


**Figure 6:** Humidity sensing response of (a) undoped and (b) Pb-doped ZnO

#### 4. CONCLUSION

Pb-doped ZnO nanostructures were successfully deposited using sol-gel immersion method. It is observed that Pb doping can alter the morphology of ZnO nanostructures and increasing the average diameter of the nanostructures. The diameter of the nanostructures was increased from 50 to 80 nm after doped. Besides, the crystallinity of the film improved after doped with Pb. Furthermore, the crystallite size of the Pb-doped film increased from 18.1 to 19.4 nm. In addition, the optical properties of the films showed excellent transmittance properties of the Pb-doped ZnO with average transmittance of 83%. The Pb-doped sample displayed better absorbance than that of undoped ZnO at UV region and high optical band gap energy of 3.27 eV. Pb-doped ZnO film showed a stable response to humidity change with a sensitivity of 1.21. Pb doping has slightly improved the performance of ZnO-based humidity sensor in humidity detection. Thus, it is suggested that Pb is suitable to be used as dopant to enhance the ZnO properties.

#### ACKNOWLEDGEMENT

The author would like to thank Faculty of Electrical Engineering, UiTM for the financial support. This work was supported by the ASEAN-India Research & Training Fellowship (IMRC/AISTDF/R&D/P-1/2017). The authors also would like to thank the Institute of Research Management and Innovation (IRMI) of UiTM for their financial support of this research

#### REFERENCES

1. B. Sarma, B.K. Sarma, "Role of residual stress and texture of ZnO nanocrystals on electro-optical properties of ZnO/Ag/ZnO multilayer transparent conductors", *Journal of Alloys and Compounds*, 734, (2018), pp.210-219.  
<https://doi.org/10.1016/j.jallcom.2017.11.028>
2. E. Przewdziecka, J.M. Sajkowski, M. Stachowicz, A. Kozanecki, "Luminescence related to two-dimensional gas in ZnO/ZnMgO heterostructures", *Thin Solid Films*, 643, (2017), pp.31-35.  
<https://doi.org/10.1016/j.tsf.2017.06.015>
3. Y. Dou, F. Wu, C. Mao, L. Fang, S. Guo, M. Zhou, "Enhanced photovoltaic performance of ZnO nanorod-based dye-sensitized solar cells by using Ga doped ZnO seed layer", *Journal of Alloys and Compounds*, 633, (2015), pp.408-414.  
<https://doi.org/10.1016/j.jallcom.2015.02.039>
4. M.H. Mamat, M.F. Malek, N.N. Hafizah, M.N. Asiah, A.B. Suriani, A. Mohamed, N. Nafarizal, M.K. Ahmad, M. Rusop, "Effect of oxygen flow rate on the ultraviolet sensing properties of zinc oxide nanocolumn arrays grown by radio frequency magnetron sputtering", *Ceramics International*, 42, (2016), pp.4107-4119.  
<https://doi.org/10.1016/j.ceramint.2015.11.083>
5. G. Nagaraju, Y.H. Ko, J.S. Yu, "Effect of diameter and height of electrochemically-deposited ZnO nanorod arrays on the performance of piezoelectric nanogenerators", *Materials Chemistry and Physics*, 149-150, (2015), pp. 393-399.  
<https://doi.org/10.1016/j.matchemphys.2014.10.034>
6. I.N. Reddy, C.V. Reddy, M. Sreedhar, M. Cho, J. Shim, V.R. Reddy, C.-J. Choi, D. Kim, "Effect of seed layers (Al, Ti) on optical and morphology of Fe-doped ZnO thin film nanowires grown on Si substrate via electron beam evaporation", *Materials Science in Semiconductor Processing*, 71, (2017), pp.296-303.  
<https://doi.org/10.1016/j.mssp.2017.08.015>
7. K. Lovchinov, G. Marinov, M. Petrov, N. Tyutyundzhiev, T. Babeva, "Influence of ZnCl<sub>2</sub> concentration on the structural and optical properties of electrochemically deposited nanostructured ZnO", *Applied Surface Science*, 456, (2018), pp.69-74.  
<https://doi.org/10.1016/j.apsusc.2018.06.088>
8. A.S. Ismail, M.H. Mamat, N.D. Md. Sin, M.F. Malek, A.S. Zoolfakar, A.B. Suriani, A. Mohamed, M.K. Ahmad, M. Rusop, "Fabrication of hierarchical Sn-doped ZnO nanorod arrays through sonicated sol-gel immersion for room temperature, resistive-type humidity sensor applications", *Ceramics International*, 42, (2016), pp.9785-9795.  
<https://doi.org/10.1016/j.ceramint.2016.03.071>
9. N. Chahmat, T. Souier, A. Mokri, M. Bououdina, M.S. Aida, M. Ghers, "Structure, microstructure and optical properties of Sn-doped ZnO thin films", *Journal of Alloys and Compounds*, 593, (2014), pp.148-153.  
<https://doi.org/10.1016/j.jallcom.2014.01.024>



10. S.A. Azzez, Z. Hassan, J.J. Hassan, M.S. Mukhlif, M.S. Mahdi, M. Bououdina, **“Effect of temperature on hydrothermally grown high-quality single-crystals Mg-doped ZnO nanorods for light-emitting diode application”**, *Journal of Luminescence*, 192, (2017), pp.634-643.  
<https://doi.org/10.1016/j.jlumin.2017.07.050>
11. M.H. Mamat, M.Z. Sahdan, Z. Khusaimi, A.Z. Ahmed, S. Abdullah, M. Rusop, **“Influence of doping concentrations on the aluminum doped zinc oxide thin films properties for ultraviolet photoconductive sensor applications”**, *Optical Materials*, 32, (2010), pp.696-699.  
<https://doi.org/10.1016/j.optmat.2009.12.005>
12. R. Yousefi, F. Jamali-Sheini, A. Sa'aedi, A.K. Zak, M. Cheraghizade, S. Pilban-Jahromi, N. Ming Huang, **“Influence of lead concentration on morphology and optical properties of Pb-doped ZnO nanowires”**, *Ceramics International*, 39, (2013), pp.9115-9119.  
<https://doi.org/10.1016/j.ceramint.2013.05.008>
13. M. Yilmaz, Ş. Aydoğan, **“The effect of Pb doping on the characteristic properties of spin coated ZnO thin films: Wrinkle structures”**, *Materials Science in Semiconductor Processing*, 40, (2015), pp.162-170.  
<https://doi.org/10.1016/j.mssp.2015.06.064>
14. M.F. Malek, M.H. Mamat, M.Z. Musa, T. Soga, S.A. Rahman, S.A.H. Alrokayan, H.A. Khan, M. Rusop, **“Metamorphosis of strain/stress on optical band gap energy of ZAO thin films via manipulation of thermal annealing process”**, *Journal of Luminescence*, 160, (2015), pp.165-175.  
<https://doi.org/10.1016/j.jlumin.2014.12.003>
15. M. Jlassi, I. Sta, M. Hajji, H. Ezzaouia, **“Effect of nickel doping on physical properties of zinc oxide thin films prepared by the spray pyrolysis method”**, *Applied Surface Science*, 301, (2014), pp.216-224.  
<https://doi.org/10.1016/j.apsusc.2014.02.045>
16. R. Mohamed, M.H. Mamat, A.S. Ismail, M.F. Malek, A.S. Zoolfakar, Z. Khusaimi, A.B. Suriani, A. Mohamed, M.K. Ahmad, M. Rusop, **“Hierarchically assembled tin-doped zinc oxide nanorods using low-temperature immersion route for low temperature ethanol sensing”**, *Journal of Materials Science: Materials in Electronics*, 28, (2017), pp.16292-16305.  
<https://doi.org/10.1007/s10854-017-7535-9>
17. A.S. Ismail, M.H. Mamat, M.M. Yusoff, M.F. Malek, A.S. Zoolfakar, R.A. Rani, A.B. Suriani, A. Mohamed, M.K. Ahmad, M. Rusop, **“Enhanced humidity sensing performance using Sn-Doped ZnO nanorod Array/SnO<sub>2</sub> nanowire heteronetwork fabricated via two-step solution immersion”**, *Materials Letters*, 210, (2018), pp.258-262.  
<https://doi.org/10.1016/j.matlet.2017.09.040>